Vapor-phase impregnation decomposition technique as an alternativeto decorate MWCNTs withPt and PdNPs for ammonia gas detection

S Capula-Colindres, G Terán, E Torres-Santillán, Khalifa Aguir, O. G. Súchil, J. C. Velázquez, J Oliva

Colloid and Interface Science Communications 44 (2021) 100490

Contents lists available at ScienceDirect

Colloid and Interface Science Communications

journal homepage: www.elsevier.com/locate/colcom

Vapor-phase impregnation decomposition technique as an alternativeto decorate MWCNTs withPt and PdNPs for ammonia gas detection

S. Capula-Colindres [a,b], G. Terán [b,c,*], E. Torres-Santillán [c], K. Aguir [d], O.G. Súchil [a], J. C. Velázquez [c], J. Oliva [e]

[a] Laboratorio de Microtecnología y Sistemas Embebidos, Centro de Investigación en Computación del Instituto Politécnico Nacional, México City 56506, Mexico
[b] Departamento de Metalurgia, IPN-CECYT2, Instituto Politécnico Nacional, México City 07738, Mexico
[c] Departamento de Ingeniería Industrial, ESIQIE, Instituto Politécnico Nacional, México City 07738, Mexico
[d] Aix-Marseille. Univ, Université de Toulon, CNRS, IM2NP, Marseille, France
[e] CONACYT-División de Materiales Avanzados, Instituto Potosino de Investigación Científica y Tecnológica A. C., 78216 San Luis Potosí, SLP, Mexico

ARTICLE INFO

Keywords:
Ammonia gas detection
Multi-walled carbon nanotubes
Interdigitated electrode
Chemiresistive sensor
Platinum
Paladium

ABSTRACT

The Vapor Phase Impregnation decomposition method (VP-IDM) is presented in this study as an alternative technique to obtain well-dispersed metallic nanoparticles on CNTs, for ammonia (NH_3) gas detection. We have analyzed the effectiveness of this method by using chemiresistive sensors (CHRs) based on multi-walled carbon nanotubes (MWCNTs) decorated with Pt and Pd nanoparticles (NPs). We measured their sensitivity through their electrical resistance variation in the presence of NH_3 gas at concentrations from 10 to 200 ppm. Pt/MWCNTs showed the highest sensitivity of about 120% at 100 ppm and 250 °C. It was revealed that the size, dispersion, temperature and type of metal NPs deposited on the MWCNTs are crucial for the detection of the NH_3 gas by the CHRs.

1. Introduction

According to the Occupational Safety and Health Administration (OSHA), ammonia gas (NH_3) is considered a toxic substance. OSHA has established the permissible exposure limit of 20 ppm during a working day of 8 h and 35 ppm for short-term exposure of 15 min. [1]. Due to its high impact on health and the environment, continuous monitoring of NH_3 is necessary. Multi-walled Carbon nanotubes (MWCNTs) are nanostructured materials with a high potential for pollutant gas detection in real-time. This nanomaterial presents interesting electrical properties, large surface area-to-volume-ratio [2,3], efficient thermal stability, and high gas adsorption capability [4–9]. The interaction between the MWCNTs obtained directly from synthesis, and NH_3 gas is weak, which affects the sensitivity and selectivity response [10]. It is possible to improve the response detection of the MWCNTs by its functionalization. This method increases the reactivity and dispersity of the material [11]. Nanoparticles (NPs) exhibit excellent physicochemical properties and have many superficial active atoms [12]. Metallic NPs decoration on MWCNTs can modify their charge transfer behavior improving the adsorption mechanism [13]. Consequently, they have a better sensitivity for the detection of toxic gases in the environment. *Nguyen* et al. [14] compared the sensitivity between MWCNTs with and without metallic NPs in the presence of ammonia gas at 70 ppm. MWCNTs decorated with Pt—Ag NPs showed up to 5% more sensitivity than the MWCNTs without NPs, which have only 1.5%. Nanoparticles such as Au, Pt [15–17] SnO_2 [18], Ag [14,19], Co [20], ITO [21], Ag/polyaniline [22] Pd [23] and CdS [10] have been also used on MWCNTs, for ammonia gas detection. So far, techniques such as electron beam evaporation, plasma treatment, sputtering coating, precipitation from the metal salt solution, and thermal evaporation have been employed to decorate MWCNTs [15–23]. Even though interesting efforts have been made to increase sensitivity and selectivity on MWCNTs, it remains a constant need to find better techniques to gain a large response with a lower response and recovery times. The vapor phase impregnation decomposition method (VP-IDM) is an alternative to obtain well-dispersed metallic nanoparticles on MWCNTs [24]. This method is similar to the Chemical Vapor Deposition (CVD) method, except that first, an organic metal precursor is mechanically incorporated in the support. Then, it is impregnated by the precursor vapor. A well-known approach for integrating MWCNTs in gas sensing applications consists

* Corresponding author at: Departamento de Ingeniería Industrial, ESIQIE, Instituto Politécnico Nacional, México City 07738, Mexico.
E-mail addresses: gerardoteranm@gmail.com, gteranm@ipn.mx (G. Terán).

https://doi.org/10.1016/j.colcom.2021.100490
Received 13 January 2021; Received in revised form 12 August 2021; Accepted 13 August 2021

in depositing the MWCNTs over a resistive substrate with interdigitated electrodes conforming a chemiresistive sensor (CHRs) and measure its electrical resistance change in the presence of a gas [25–27].

Therefore, in our present study, we have implemented the VP-IDM as a new alternative method to decorate MWCNTs with Pd and Pt NPs for Ammonia gaseous sensing applications. The sensitivity to different ammonia gas concentrations and temperatures was evaluated by integrating the decorated MWCNTS on the CHRs.

2. Materials and methods

2.1. Multi-walled CNTs decoration process

The MWCNTs were produced by Chemical Vapor Deposition (CVD) [28] and purified by an oxidizing process using a mixture of HNO_3 and H_2SO_4 (1:3 ratio), described in-depth in a previous paper [29]. The MWCNTs were decorated with Pt and Pd NPs by implementing a vapor phase impregnation decomposition technique (VP-IDM) [24]. Pd and Pt acetylacetonates (Pt $(acac)_2$, Pd $(acac)_2$) were used as precursors. In the first step, the metallic NPs and MWCNTs were mechanically mixed for 15 min. The metallic deposition was carried out until an increase of 3% in the weight of the MWCNTs was obtained. Secondly, the mixture was placed inside a horizontal quartz-tube at 180 °C for 10 min. (at a pressure of 500 Torr). After this, the temperature of the quartz-tube was increased to 400 °C and maintained 10 min at this temperature in order to decompose the precurso's vapors.

The prepared nanocomposites of Pt/MWCNTs or Pd/MWCNTs were dispersed in glycerol using sonication for 1 h. We have deposited the nanocomposites on silicon substrates to fabricate a CHRs based on Pt/Pd MWCNTs for ammonia gas detection. For this, a droplet of solution containing Pt/MWCNTs or Pd/MWCNTs was dropped on the Pt metalized interdigitated electrodes of the CHRS and dried at 400 °C for 2 h.

2.2. Gas detection measurements

The shift in electrical resistance of the Pt/MWCNTs or Pd/MWCNTs nanocomposites deposited on the interdigitated electrodes of the CHRs was measured first by varying the concentration of ammonia gas (20, 60 and, 100 ppm) with a constant flow and at room temperature. Later, the process was repeated but varying the sensor's operating temperature (25, 120, and 250 °C), which was sensed by a thermopar and set with a Temperature controller. The CHRs were placed in a sealed stainless test cell (located at the center on Fig. 1). Then exposed for 30 s to a mixture (air+NH_3) using the mass flow controllers of 500 ml/min depicted on the left side of Fig. 1. The electrical resistance was measured with a Keithley 6430 digital multi-meter connected to a PC for data acquisition, as observed in the right side of Fig. 1.

The crystallographic structure of the MWCNTs was analyzed through X-ray diffraction measurements using a PANalytical-790 AC X'Pert Pro with a Cu Kα radiation and a wavelength of 1.54 Å. The morphology of the MWCNTs was examined using transmission electron microscopy (TEM), JEM 2100, with an accelerating voltage of 200 kV.

3. Theory

3.1. CHRs sensitivity calculation and determination of the response/recovery times

The CHRs sensitivity *(S%)* was estimated according to the following equation:

$$S(\%) = \frac{(R_g - R_0)}{R_0} * 100 \quad (1)$$

Where R_0 is the initial resistance of the sensor before gas exposure and Rg is the value of resistance produced by the sensor during its exposure to the ammonia (NH_3) gas [30]. For this investigation, we defined the response time as the time required to reach the minimum value of the sensor's resistance (minimum peak resistance) with respect to a base line level (reference resistance R_0) during the NH_3 exposure and the recovery time is defined as the time required to increase the resistance value until the reference base line level.

4. Results and discussion

4.1. Crystal structure of MWCNTs

The XRD patterns obtained from MWCNTs with and without functionalization are observed in Fig. 2(a,b). In Fig. 2(a), the most intense diffraction peak for the non-functionalized MWCNTs was located at 26.32°, followed by a weak diffraction peaks for the planes (002), (100), and (101). These peaks correspond to 2H graphite (JCPDS-089-7213). The agreement between the MWCNTs and graphite diffraction patterns is often given by the intrinsic properties of the graphene [31]. On the other hand, Fig. 2(b) shows the diffraction peaks for the functionalized MWCNTs, which are broader and less intense than these in Fig. 2(a). The variation in results might be caused by tension between the graphite layers and a decreasing number of walls in the MWCNTs during the oxidation process [32,33]. By analyzing only the diffraction peak of the (002) plane in both samples, it was observed that the peak is slightly displaced to the left for the functionalized MWCNTs. This effect is given due to the elimination of impurities, mostly of carbon present at the nanotube walls. It was also observed that the diameter decreases by the loss of walls that form the MWCNTs [34,35].

As observed in Fig. 3(a), the MWCNTs without functionalization are

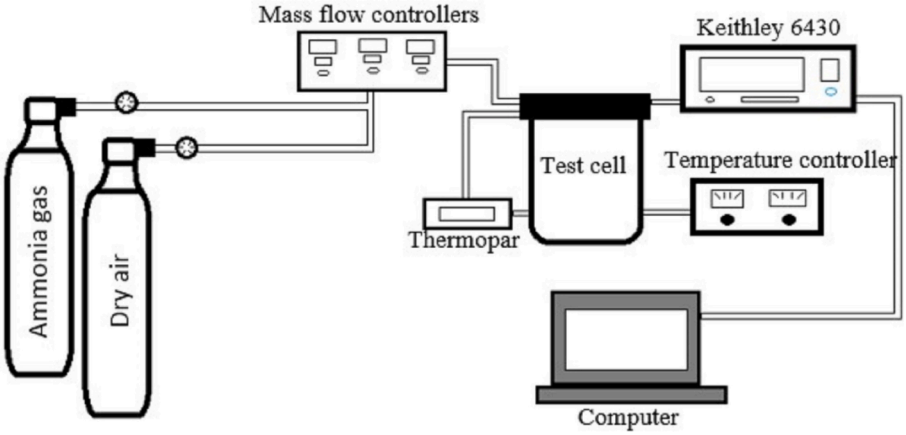

Fig. 1. Schematic of the experimental setup for the ammonia gas detection.

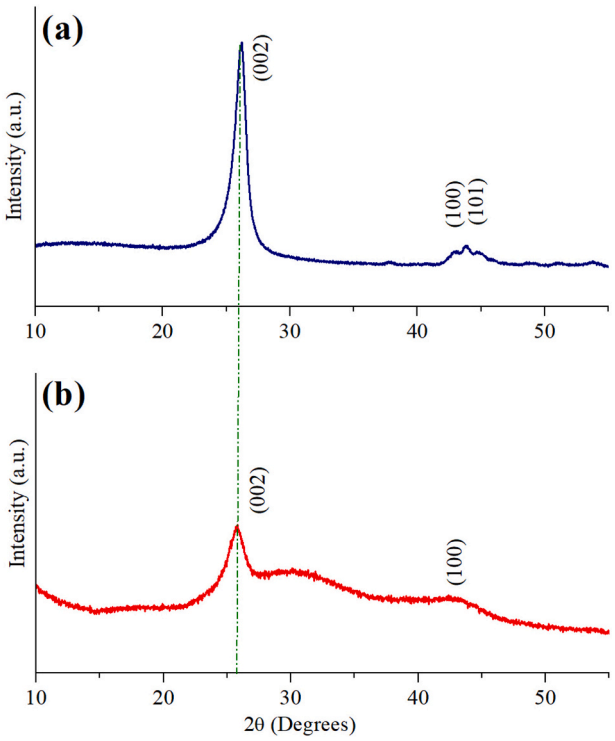

Fig. 2. XRD diffraction patterns and TEM images from samples of MWCNTs. The MWCNTs non-functionalized are depicted in (a) and functionalized (b), respectively.

interconnected forming an entangled network. This phenomenon is caused by high Van der Waals forces among tubes [36]. Carbon nanotubes show average diameters of 43.1 ± 30 nm (Fig. 3b-c). In the same figure, it is observed the multi-walled nature of nanotubes. The spacing between the walls was 0.36 nm, see Fig. 3(c). Then, after the MWCNTs were functionalized, they showed a decrease in diameters down to 18 ± 25 nm, as observed for the sample in Fig. 3(d-f). This decrease in the nanotube walls showed an agreement with the XRD patterns results, as mentioned in the previous section. Besides, it was also observed for other functionalized MWCNTs an alteration in their walls, see Fig. 3(d). This alteration might be attributed to defects and the introduction of functional groups (Carboxylic (-COOH), carbonyl (-C=O), and hydroxyl (-OH)). The functional groups are frequently found on the surfaces of MWCNTs after oxidation treatments and act as efficient adsorption sites that promote the dispersion and nucleation of noble metal particles on MWCNTs [37].

4.2. Morphologic analysis of decorated MWCNTs

The comparison between MWCNTs decorated with Pt and Pd NPs is observed in Fig. 4 (a-f). The statistical analysis was carried out to obtain the mean and non-parametric variance of the NPs sizes. The size results of the NPs are shown in the Table 1. We observed that the statistical distribution of sizes for both types of NPs was different. According to *Muratore* et al. [38], the difference between sizes relies on the cohesion energy (E_{coh}) of the metal. Thus, metals with high cohesion energy (E_{coh}) exhibits small particle sizes and high particle densities. Consequently, given that Pt and Pd have E_{coh} values of 5.88 eV and 3.64 eV [39], we found a significant correlation between their E_{coh} and particle size. Both types of NPs exhibited mainly spherical shape (see Fig. 4(a,b)). The measured interplanar distances of Pt and Pd NPs were 0.225 and 0.22 nm (see Fig. 4(c,d)), corresponding to an FCC crystal of Pt and Pd (JCPDS cards 04–0802 and 00–046-1043).

From the statistical analysis, we found that the Pt NPs have a lower variance value than Pd NPs. To support this statement, we computed a statistical distribution and fit two histograms with a LogNormal scale using the three parameters Kolmogorov-Smirnov test, as shown in Fig. 4 (e,f) [40,41]. Afterward, we found that Pd NPs sizes have a more homogeneous and almost Gaussian distribution than Pt NPs.

Pt NPs showed a more heterogeneous dispersion on the MWCNTs surface, as observed in Fig. 4(a). It was found a high accumulation of the NPs in some regions. This effect has an agreement with the one observed in Titania nanotubes reported by *Encarnación* et al. [42]. It was attributed to a low metallic charge (1 to 3%) and a preference for diffusion to regions with a low demand of saturation for the OH groups. Thus, a lower variance as the one observed for Pt NPs can also be interpreted as a lower density of NPs per unit of area caused by a poor homogeneity in the MWCNTs surface distribution. Fig. 4(g) shows the energy-dispersive X-ray (EDX) spectra of MWCNTs decorated with Pt NPs. The presence of Pt peaks are evident, confirming that the nanocomposites contain this

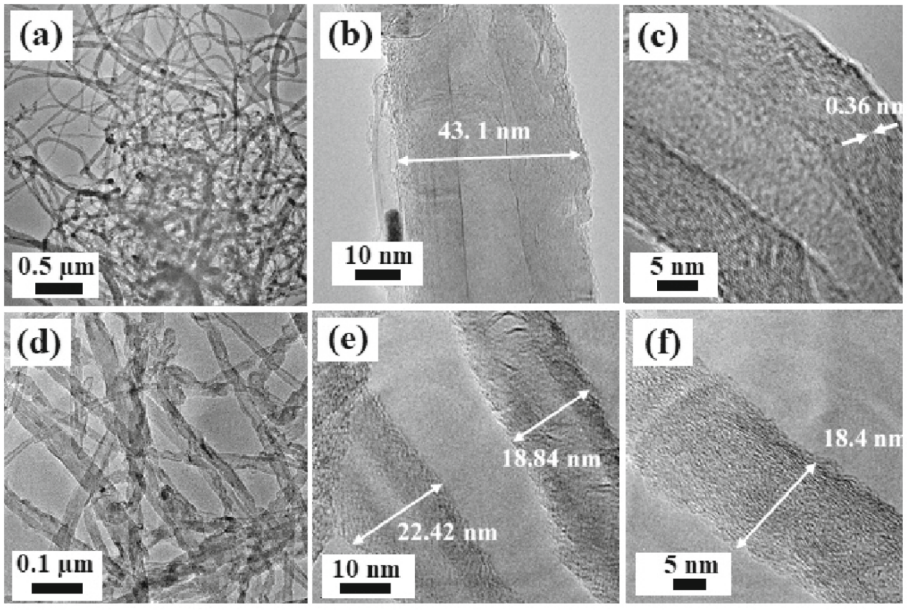

Fig. 3. TEM images of the non-functionalized (a-c) and functionalized (d-f) MWCNTs at different magnifications.

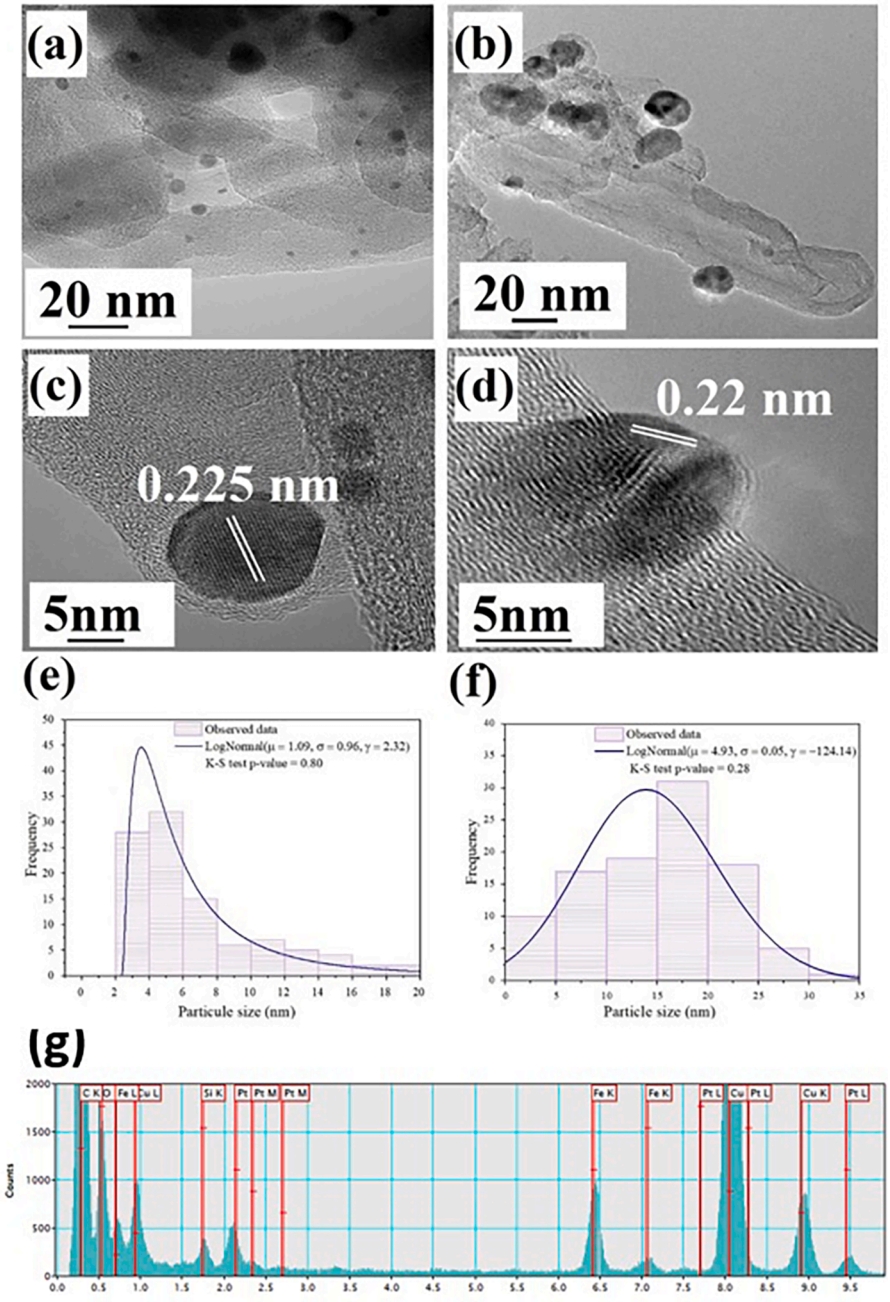

Fig. 4. TEM images of the MWCNTs decorated with Pt in (a,c) and Pd in (b,d) are shown. The Pt and Pd nanoparticle distribution histograms are depicted in (e) and (f). EDX spectra of Pt NPs is showed in (g).

Table 1
Statistical results of size for the Pt and Pd NPs.

Metal	Mean size (nm)	Variance size (nm^2)
Pt	6.85	17.64
Pd	14.82	46.58

element. Additionally, Cu, Fe and Si peaks are present in the sample but in smaller quantities. This contamination came from the grid employed to analyze the sample by TEM.

4.3. Results of the sensitivity measurement of the CHRs

Two Pt interdigitated electrodes conform the chemical resistive sensor devices, see Fig. 5 (a) and (b). The electrodes were deposited by pulverization over a silicon substrate, see the sensor's architecture in Fig. 5c. For the activation of the sensitive nanomaterial (Pd or Pt/MWCNTs) on the chemiresistive sensor surface, the drop coating method was employed. As observed in Fig. 5(d), the deposited Pt/MWCNTs or Pd/MWCNTs nanocomposites tend to accumulate at the substrate's edges. This phenomenon is known as the "coffee ring effect" generated by the consecutive evaporation and replacement of material until reaching a limit that creates a stain with a "ring-like" shape [43].

All CHRs showed an increase in their electrical resistance in the presence of the ammonia gas. This effect occurred because it is a reducing gas and causes an electron donation to the conduction band of the sensitive material after the adsorption of the gas molecules [30,44,45]. The change of resistance in the sensors suggests that they are sensitive to the ammonia gas. We measured the sensitivity of the Pd/

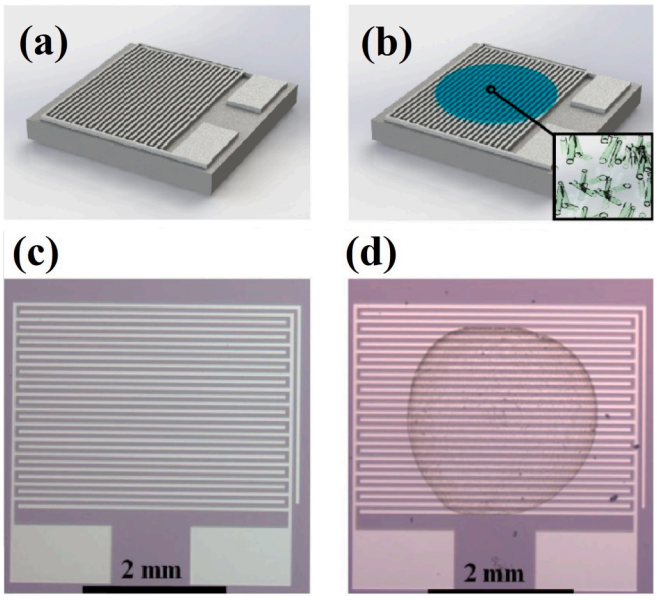

Fig. 5. 3D representation and Optical top view images of the chemiresistive sensor (CHRs) before (a,c) and after (b,d) the MWCNTs were deposited over the surface.

MWCNTs and Pt/MWCNTs for the detection of NH_3 separately, see Fig. 6 (a,b). First, the concentrations of NH_3 was varied from 10 ppm to 200 ppm with a fixed room temperature and constant gas flow. Subsequently, in a second test, we changed the temperature of the sensor (operating temperature) to 25 °C, 120 °C, and 250 °C for each gas concentration.

From these results, we found the highest sensitivity at 250 °C for the Pt/MWCNTs based sensor, see Fig. 6(c). The cycles of NH_3 detection for the Pt/MWCNTs based sensor are shown in Fig. 6(d). When the sensor is exposed to the NH_3 (gas-in), an abrupt decrease of resistance occurred. Later, the gas flow is stopped (gas-out) and the resistance increases again

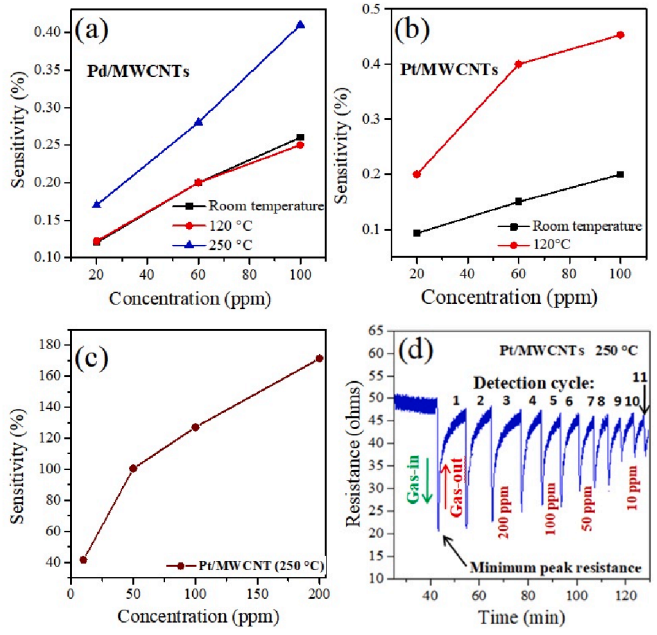

Fig. 6. The sensitivity of the CHRs with Pd and Pt at different temperatures is shown in (a and b). In (c), the best results for the Pt/MWCNTs sensor at 250 °C is observed. The performance of the Pt/MWCNTs sensor for different concentrations is depicted in (d).

reaching the original base line level. This is considered as one cycle of detection for the NH_3 gas and several cycles were carried out to detect NH_3 with different concentrations of 200 ppm (cycles 1–3), 100 ppm (cycles 4–6), 50 ppm (cycles 7 and 8) and 10 ppm (cycles 9–11). The response/recovery times were calculated from these detection cycles and the results were summarized in the Table 2.

From the table above, we infer that our values of sensitivity (41–171.5) for the sensor containing Pt/MWCNTs (at 250 °C) are much higher than these previously reported in literature (0.025–10) for CNT based systems decorated with other metallic NPs. According to *Young and Lin* et al. [16,17], Au NPs can give a range of sensitivity from 1.1 to 2.74%. Other cases, such as Ag/MWCNT sensors reported by *Nguyen* et al. [14] and *Cui* et al. [19] showed a sensitivity of 9% at room temperature. For our particular case, the Pd/MWCNTs sensors at room temperature can be compared to those reported by *Choi* et al. [23], showing an average sensitivity of 0.20% for concentrations from 20 to 100 ppm. Similarly, the Pt/MWCNTs sensors also showed a low average sensitivity of 0.15% at room temperature, but it increases to 171% at 250 °C. In addition, we observed that our sensors tested at room temperature had recovery time of several minutes, while the sensor made with Pt/MWCNTs and tested at 250 °C had a lower recovery time of 40 s. Thus, a higher operating temperature in the sensor produces higher sensitivity and higher response time, compare the values of response time for the Pt/MWCNT based sensor tested at room temperature with that for the sensor tested at 250 °C, see Table 2. It is worthy to mention that the sensors containing Pt/MWCNT are better for the NH_3 detection than these made with Pd/MWCNT because their response time are lower, compare their response time at room temperature in Table 2. According to *Abdulla* et al. [22], the high binding energy (E_b) between the ammonia gas molecules, the defects present on the MWCNTs surface, and the absorbed oxygen could considerably increase the recovery time of the sensor at room temperatures. Furthermore, *Van* et al. [18] found that composites of SnO_2/MWCNTs increase their sensitivity for the detection of the ammonia gas when high operating temperatures are employed, since this causes the desorption of the gas molecules from the surface of the MWCNTs. For this last reason, our sensors had lower recovery times at higher operating temperatures.

Fig. 7 shows the values of sensitivity for our best Pt/MWCNT based sensor as a function of the NH_3 concentration as well as for other previous reported sensors. It is observed that the Pt/MWCNTs sensor fabricated in this work has and operated at 250 °C had superior values of sensitivity in comparison with the previous publications. In general, the sensitivity value is directly proportional to the increase of the ammonia concentration.

The method to decorate the CNTs with different metallic NPs as well as the density, dispersion, surface functionalization and size of the metallic nanoparticles had a strong influence on the sensitivity of the sensors. The process of functionalization for the CNTs determines the reactivity, the mechanical and electrical behavior of the CNTs [46]. The functionalization introduces functional groups on the CNTs surface, increasing wettability, hydrophobicity, and gas absorption [37,47]. The internal defects present at the CNTs surface might serve as nucleation sites or anchors for the incorporation of NPs [48,49]. The nucleation sites are responsible for the size and dispersion of the NPs. *Mendoza* et al. [50] suggested that a high density of defects can be interpreted as an increased number of preferred adsorption sites for different types of gases. These defects can change the interaction between the NPs and the CNTs [51].

According to *Chang* et al. [4], it was reported for single-walled CNTs (SWCNTs) that the gaseous ammonia adsorption showed low binding energy and can be supported in the density functional theory. However, when metallic NPs are incorporated on the surface of a nanotube, this binding energy is modified, improving the sensitivity response. They found a relationship between the amount of binding energy (E_b) and electron charge transfer. This relationship is intrinsically linked to the sensitivity response. By focusing only on the role of the NPs size, it has

Table 2
Sensitivity for sensors based on MWCNTs decorated with metallic NPs to detect ammonia gas.

Material	Metallic Load Thickness (nm)	Decoration method	S(%)	T(°C)	Concentration (ppm)	Response time (s)	Recovery time (s)	Ref.
Au/CNT	5	Electron beam	1.1	Room. T.	50	–	–	[16]
			2.74		800			
Pt/MWCNT	4	Evaporation	3	Room. T.	70	50	300	[14]
Ag/MWCNT			6.9		70		500	
Au/MWCNT	5	Electron beam	1.6	Room. T.	50	–	–	[17]
			5.4		800			
Ag/MWCNT	–	Mini-arc plasma	2.8	Room. T.	1% NH_3	7	Several mins.	[19]
			9.0		8% NH_3			
Pd/CNT	–	Impregnation	0.025	Room. T.	7	8 to 16	–	[23]
			0.20		35			
Co/MWCNT	2	Sputtering	1.5	Room. T.	14	30 to 50	200 to 500	[20]
			4.3		800			
CdS/ MWCNT	–	Chemical precipitation	10	Room. T.	100	61	60	[10]
Pt/MWCNT	3 wt%	VP-IDM	0.097	Room. T.	20	12 to 14	Several mins.	This work
			0.157		60			
			0.198		100			
			41.52	250	10	24 to 33	40	
			100.34		50			
			127		100			
			171.5		200			
Pd/MWCNT			0.129	Room. T.	20	69 to 78	Several mins.	
			0.215		60			
			0.266		100			

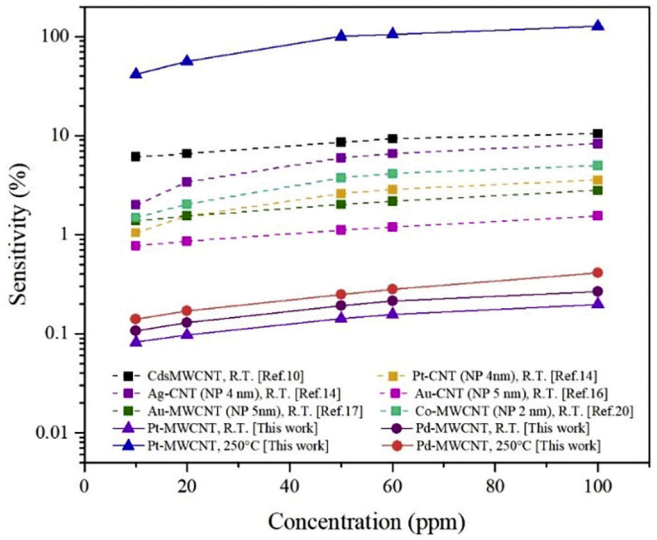

Fig. 7. Comparison of the sensitivity value of different systems using metallic NPs and MWCNTs.

been reported by *Randeniya* et al. [45] that Au NPs with a length of less than 3 nm exhibit a higher sensitivity response. *Li* et al. [52] also reported for Pt/CNTs that the sensitivity properties can be related to the nanoparticle size and distribution on the surface.

By considering these previous results, we have observed that the sensitivity increased with smaller sizes of NPs. This increase maximizes the effect of adsorbents on metal clusters. The NPs size is dependent on catalytic activity [53] and, the density of NPs over the CNTs surfaces influences the sensing response dramatically [52]. Additionally, it was observed that the larger is the metallic load deposited over the CNT's surface, the more significant number of reactive locations may interact with the ammonia gas molecule, increasing the sensitivity response of the CHRS consequently. Another factor to be considered in the sensor response to NH_3 detection is relative humidity (RH). *Rigoni* et al. [54] performed a study using functionalized SWCNTs with carboxylic acid (COOH) and cetyltrimethyl ammonium bromite (CTAB) at different RH values. Both samples exhibited an increase sensitivity response to ammonia as the percentage of relative humidity increases. *Liu* et al. [55] claimed that the resistance of MWCNTs increases with the increase of % RH.

5. Conclusions

Two different Chemiresistive sensors were fabricated based on MWCNTs decorated with Pd and Pt NPs by vapor-phase impregnation decomposition method. Both sensors were able to detect ammonia gas at different concentrations and temperatures. We found that Pd/MWCNTs exhibited the best sensitivity at room temperature, and at 250 °C, Pt/MWCNTs showed the best sensitivity. We have seen that the type of metal deposited, the temperature, and the size of the NPs played an essential role in fast ammonia gas detection. We observed that with a smaller NPs size, larger is the reactivity of the sensor. We related the size of the NPs with a larger number of active sites, having, in consequence, more considerable gas adsorption. We observed the level of dispersion between NPs through TEM images, and we found that CNTs decorated with Pt NPs have a higher dispersion than those with Pd NPs.

Declaration of competing interest

The authors declare no conflict of interest.

Acknowledgments

The authors would like to acknowledge Consejo Nacional de Ciencia y Tecnología (CONACyT) and Instituto Politécnico Nacional (IPN) for financial support throughout this research: IPN-SIP 20180507. The authors are grateful to Felipe Cervantes Sodi, Universidad Iberoamericana for assistance with MWCNT synthesis and T.Fiorido, Institut Matériaux Microélectronique et Nanosciences de Provence (IM2NP), for gas measurements support.

References

[1] Agency for Toxic Substances & Disease Registry (ATSDR), Toxic Substances Portal-Ammonia. https://www.atsdr.cdc.gov/phs/phs.asp?id=9&tid=2, 2004 (Accessed 12 January 2019).
[2] X. Zhang, X. Hou, D. Pan, B. Pan, L. Liu, B. Chen, K. Kondoh, S. Li, Designable interfacial structure and its influence on interface reaction and performance of

MWCNTs reinforced aluminum matrix composites, Mater. Sci. Eng. A 139783 (2020), https://doi.org/10.1016/j.msea.2020.139783.
[3] S. Fu, X. Chen, P. Liu, Preparation of CNTs/cu composites with good electrical conductivity and excellent mechanical properties, Mater. Sci. Eng. A 771 (2020) 138656, https://doi.org/10.1016/j.msea.2019.138656.
[4] H. Chang, J.L. Do, S.L. Mi, Y.L. Hee, Adsorption of NH_3 and NO_2 molecules on carbon nanotubes, Appl. Phys. Lett. 79 (23) (2001) 3863–3865, https://doi.org/10.1063/1.1424069.
[5] S. Manivannan, L.R. Shobin, A.M. Saranya, B. Renganathan, D. Sastikumar, P. K. Chang, Carbon nanotubes coated fiber optic ammonia gas sensor, in: Proceeding of the Conference SPIE Integrated Optics: Devices, materials and technologies XV, 2011, pp. 79410M.1–79410M.7. San Francisco, California, United States.
[6] E.S. Torres, S.C. Capula, CMSG, N.C. Cayetano Reza, E.C. Villagarcía, Effect of functional groups in the structure of carbon nanotubes to adsorption grade of cadmium ions, Rev. Mex. Ing. Quím. 17 (3) (2018) 955–961, https://doi.org/10.24275/uam/izt/dcbi/revmexingquim/2018v17n3/Torres.
[7] V.M. Aroutiounian, Metal oxide gas sensors decorated with carbon nanotubes, Lith. J. Phys. 55 (4) (2015) 319–329, https://doi.org/10.3952/physics.v55i4.3230.
[8] H. Baccar, A. Thamri, P. Clement, E. Llobet, A. Abdelghani, Beilstein, Pt and Pd decorated MWCNTs for vapour and gas detection at room temperature, J. Nanotech 6 (2015), https://doi.org/10.3762/bjnano.6.95, 919–917.
[9] P. Slobodian, P. Riha, A. Lengalova, P. Svoboda, P. Saha, Multi-wall carbon nanotube networks as potential resistive gas sensors for organic vapor detection, Carbon N. Y. 49 (2011) 2499–2507, https://doi.org/10.1016/j.carbon.2011.02.020.
[10] S.T. Hasnahena, M. Roy, Sensing of low concentration of ammonia at room temperature by cadmium sulphide nanoparticle decorated multi-walled carbon nanotube: fabrication and characterization, J. Phys. D. Appl. Phys. 50 (2017) 505103, https://doi.org/10.1088/1361-6463/aa94f2.
[11] V. Datyuk, M. Kalyva, K. Papagelis, J. Parthenios, D. Tasis, A. Siokou, I. Kallitsis, C. Galiotis, Chemical oxidation of multi-walled carbon nanotubes, Carbon 46 (2008) 833–840, https://doi.org/10.1016/j.carbon.2008.02.012.
[12] K.S. Ashok, Engineered nanoparticles, structure, properties and mechanisms of toxicity. Chapter 4, in: Experimental Methodologies the Characterization of Nanoparticles, Academic Press, 2016, pp. 125–170.
[13] H. Lee, S. Lee, D.H. Kim, D. Perello, Y.J. Park, S.H. Hong, M. Yun, S. Kim, Integrating metal-decorated CNT networks with CMOS readout in a gas sensor, Sensor 12 (3) (2012) 2582–2597, https://doi.org/10.3390/s120302582.
[14] L.Q. Nguyen, T.P. Thanh, D.V. Truong, P.T. Kien, N.C. Tu, L.H. Bac, D.D. Vuong, N. D. Chien, N.H. Lam, Pt and Ag decorated carbon nanotubes network layers for enhanced NH_3 gas sensitivy at room temperature, Mater. Trans. 56 (9) (2015) 1399–1402, https://doi.org/10.2320/matertrans.MA201538.
[15] M. Penza, G. Cassano, R. Rossi, M. Alvisi, A. Rizzo, M.A. Signore, Enhancement of sensitivity in gas chemiresistors based on carbon nanotube surface functionalized with noble metal (Au, Pt) nanoclusters, Appl. Phys. Lett. 90 (2017) 173123, https://doi.org/10.1063/1.2722207.
[16] S.J. Young, Z.D. Lin, Ammonia gas sensors with Au-decorated carbon nanotubes, Microsyst. Technol. 24 (2018) 4207–4210, https://doi.org/10.1007/s00542-018-3712-x.
[17] Z.D. Lin, S.J. Young, Carbon nanotube thin films functionalized via loading of Au nanoclusters for flexible gas sensors devices, IEEE Trans. Electron Dev. 63 (1) (2016) 476–479, https://doi.org/10.1109/TED.2015.2504105.
[18] N.H. Van, L.T. Bich, N. Duc, Highly sensitive thin film NH_3 gas sensor operating at room temperature based on SnO_2/MWCNTs composite, Sensors Actuators B 129 (2008) 888–895, https://doi.org/10.1016/j.snb.2007.09.088.
[19] S. Cui, H. Pu, F. Lu, Z. Wen, E.C. Mattson, C. Hirschmug, M.G. Josifovska, M. Weinert, J. Chen, Fast and selective room temperature ammonia gas sensors using silver nanocrystal functionalized carbon nanotubes, Appl. Mater. Interfaces 4 (2012) 4898–4904, https://doi.org/10.1021/am301229w.
[20] L.Q. Nguyen, P.Q. Phan, H.N. Duong, C.D. Nguyen, L.H. Nguyen, Enhancement of NH_3 gas sensitivity at room temperature by carbon nanotube based sensor coated with Co nanoparticles, Sensors 13 (2013) 1754–1762, https://doi.org/10.3390/s130201754.
[21] F. Rigoni, G. Drera, S. Pagliara, A. Goldoni, L. Sangaletti, High sensitivity, moisture selective, ammonia gas sensors based on single walled carbon nanotubes functionalized with indium tin oxide nanoparticles, Carbon 80 (2014) 356–363, https://doi.org/10.1016/j.carbon.2014.08.074.
[22] S. Abdulla, D.V. Ponnuvelu, B. Pullithadathil, Rapid, trace level ammonia gas sensor based surface engineered ag nanoclusters@polyaniline/multi-walled carbon and insights into their mechanistic pathways, Chem. Select 2 (2017) 4277–4289, https://doi.org/10.1002/slct.201700459.
[23] H.H. Choi, J. Lee, K.-Y. Dong, B.K. Ju, W. Lee, Noxious gas detection using carbon nanotubes with Pd nanoparticles, Nanoscale Res. Lett. 6 (605) (2011) 1–6, https://doi.org/10.1186/1556-276X-6-605.
[24] C. Encarnación, J.R. Vargas, J.A. Toledo, M.A. Cortes, C. Angeles, Pt nanoparticles on titania nanotubes prepared by vapor phase impregnation decomposition method, J. Alloys Compounds 495 (2010) 458–461, https://doi.org/10.1016/j.jallcom.2009.10.232.
[25] N. Roy, R. Sinha, T.T. Daniel, H.B. Nemade, T.K. Mandal, Highly sensitive room temperature CO gas sensor based on MWCNT-PDDA composite, IEEE Sensors J. 1748 (2020), https://doi.org/10.1109/jsen.2020.3004994, 1–1.
[26] D. Wong, O. Abuzalat, S. Mostafa, S.S. Park, S. Kim, Intense pulsed light-based synthesis of hybrid TiO2-SnO_2/MWCNT doped cu-BTC for room temperature ammonia sensing, J. Mater. Chem. C 8 (2020) 7567–7574, https://doi.org/10.1039/d0tc00762e.
[27] G. De Pascali, D. Melisi, M. Valentini, A. Valentini, M.A. Nitti, R. Nasi, G. Casamassima, P.F. Ambrico, A. Cardone, Spray deposited carbon nanotubes for organic vapor sensors, Microelectron. J. 45 (2014) 1691–1694, https://doi.org/10.1016/j.mejo.2014.09.007.
[28] R. Andrews, D. Jacque, A.M. Rao, F. Derbyshire, D. Qian, X. Fan, E.C. Dickey, J. Chen, Continuous production of aligned carbon nanotubes: a step closer to commercial realization, Chem. Phys. Lett. 303 (1999) 467–474, https://doi.org/10.1016/S0009-2614(99)00282-1.
[29] S. Capula, K. Aguir, F. Cervantes, L. Villa, J. Moncayo, F. Garibay, Ozone sensing based on palladium decorated carbon nanotubes, Sensors 14 (2014) 6806–6818, https://doi.org/10.3390/s140406806.
[30] B. Ghaddab, J.B. Sanchez, C. Mavon, M. Paillet, R. Parret, A.A. Zahab, J. L. Bantignies, V. Flaud, E. Beche, F. Berger, Detection of O_3 and NH_3 using hybrid thin dioxide/carbon nanotubes sensors: influence of materials and processing on sensors sensitivity, Sensors Actuators B Chem. 170 (2012) 67–74, https://doi.org/10.1016/j.snb.2011.01.044.
[31] T. Belin, F. Epron, Characterization methods of carbon nanotubes: a review, Mater. Sci. Eng. B 199 (2005) 105–118, https://doi.org/10.1016/j.mseb.2005.02.046.
[32] H.K. Misak, R. Asmatulu, M. O'Malley, E. Jurak, S. Mall, Functionalization of carbon nanotube yard by acid treatment, Int. J. Smart Nano Mater. 5 (1) (2014) 34–43, https://doi.org/10.1080/19475411.2014.896426.
[33] B.C. Dong, B.N. Quoc, L.N. Thu, V.N. Quoc, T.L. Van, N.N. Huu, The impact of different multi-walled carbon nanotubes on the X-band microwave absorption of their epoxy nanocomposites, Chem. Cent. J. 9 (10) (2015) 1–13, https://doi.org/10.1186/s13065-015-0087-2.
[34] D.K. Singh, P.K. Lyer, P.K. Giri, Diameter dependence of interwall separation and strain in multi-walled carbon nanotubes probed by X-ray diffraction and Raman scattering studies, Diam. Relat. Mater. 19 (10) (2010) 1281–1288, https://doi.org/10.1016/j.diamond.2010.06.003.
[35] R. Das, S. Bee Abd Hamid, E. Ali, S. Ramakrishna, W. Yongzhi, Carbon nanotubes characterization by X-ray powder diffraction-A review, Curr. Nanosci. 11 (1) (2015), https://doi.org/10.2174/1573413710666140818210043.
[36] N. Asari, J.P. Tessonner, A. Rinaldi, S. Reiche, M.G. Kutty, Chemically modified multi walled carbon nanotubes (MWCNTs) with anchored acidic groups, Sains Malaysiana 41 (5) (2012) 603–609.
[37] P.C.P. Watts, N. Mureau, Z. Tang, Y. Miyajima, The importance of oxygen containing defect on carbon nanotubes for the detection of polar and non-polar vapours through hydrogen bond formation, Nanotechnology 18 (17) (2007) 175701, https://doi.org/10.1088/0957-4484/18/17/175701.
[38] C. Muratore, A.N. Reed, J.E. Bultman, S. Ganguli, B.A. Cola, A.A. Voevodin, Nanoparticle decoration of carbon nanotubes by sputtering, Carbon 57 (2013) 274–281, https://doi.org/10.1016/j.carbon.2013.01.074.
[39] A. Maiti, A. Ricca, Metal-nanotube interactions binding energies and wetting properties, Chem. Phys. Lett. 395 (2004) 7–11, https://doi.org/10.1016/j.cplett.2004.07.024.
[40] F.M. Dekking, C. Kraaikamp, H.P. Lopuhaa, L.E. Meester, A modern introduction to probability and statistics-understanding why and how, Springer (2005), https://doi.org/10.1007/1-84628-168-7.
[41] EasyFit-Distribution Fitting Software, Version 5.6. Math Wave Technologies, 2015 (Available online: www.mathwave.com (accessed on 12 December 2017)).
[42] C. Encarnación, M.A. Cortés, A.K. Medina, C. Angeles, M.G. Hernández, I. Cuauhtémoc, J.G. Hernández, E. López, J.R. Vargas, J.A. Toledo, Uniformly sized Pt nanoparticles dispersed at high loading on Titania nanotubes, Appl. Catal. A General 117631 (2020), https://doi.org/10.1016/j.apcata.2020.117631.
[43] R. Liu, R.L. Haiyan, H. Ding, J. Lin, F. Shen, Z. Cui, T. Zhang, Fabrication of platinum decorated single walled carbon nanotube based hydrogen sensors by aerosol jet printing, Nanotechnology 23 (50) (2004) 505301, https://doi.org/10.1088/0957-4484/23/50/505301.
[44] M. Penza, M. Rossi, M. Alvisi, G. Cassano, E. Serra, Functional characterization of carbon nanotube networked films functionalized with tuned loading of au nanoclusters for gas sensing applications, Sensors Actuators B Chem. 140 (1) (2009) 176–184, https://doi.org/10.1016/j.snb.2009.04.008.
[45] L.K. Randeniya, P.J. Martin, A. Bendavid, J. McDonnell, Ammonia sensing characteristics of carbon nanotube yarns decorated with nanocrystalline gold, Carbon 49 (15) (2011) 5265–5270, https://doi.org/10.1016/j.carbon.2011.07.044.
[46] F. Mercuri, A. Sgamellotti, Theoretical investigations on the functionalization of carbon nanotubes, Inorg. Chim. Acta 360 (2007) 785–793, https://doi.org/10.1016/j.ica.2006.07.066.
[47] X. Zhang, H. Cui, Y. Gui, J. Tang, Mechanism and application of carbon nanotube sensors in SF6 decomposed production detection: a review, Nanoscale Res. Lett. 12 (177) (2017) 1–12, https://doi.org/10.1186/s11671-017-1945-8.
[48] S. Santra, A.K. Sinha, S.K. Ray, F. Udrea, J.W. Gardner, P.K. Guha, Ambient temperature carbon nanotube ammonia sensor on CMOS platform, Procedia Eng. 87 (2014) 224–227, https://doi.org/10.1016/j.proeng.2014.11.627.
[49] J.J. Adjizian, P. De Marco, I.M. Suarez, A.A. El Mel, R. Snyders, R.Y.N. Gengler, P. Rudolf, X. Ke, G. Van Tendeloo, C. Bittencourt, C.P. Ewels, Platinum and palladium on carbon nanotubes: experimental and theorical studies, Chem. Phys. Lett. 571 (2013) 44–48, https://doi.org/10.1016/j.cplett.2013.03.079.
[50] E. Mendoza, J. Rodriguez, Y. Li, Y.Q. Zhu, C.H.P. Poa, S.J. Henley, A.R.R. Romano, J.R. Morante, S.R.P. Silva, Effect of the nanostructure and surface chemistry on the gas adsorption properties of macroscopic multi-walled carbon nanotube ropes, Carbon 45 (2007) 83–88, https://doi.org/10.1016/j.carbon.2006.08.001.
[51] C. Bittercourt, A. Felten, B. Douhard, J.F.F. Colomer, G. VanTendeoo, W. Drube, J. Ghijsen, J.J. Pireaux, Metallic nanoparticles on plasma treated carbon

nanotubes: nano2Hybrids, Surf. Sci. 601 (2007) 2800–2804, https://doi.org/10.1016/j.susc.2006.12.045.
[52] X. Li, X. Liu, W. Wang, I. Li, X. Lu, High loading Pt nanoparticle on functionalization of carbon nanotubes for fabricating nonenzyme hydrogen peroxide sensor, Biosens. Bioelectron. 59 (2014) 221–226, https://doi.org/10.1016/j.bios.2014.03.046.
[53] F. Fuchs, A.L. Zienert, C. Wagner, S. Schuster, S.E. Schulz, Interaction between carbon nanotubes and metals: electronic properties stability and sensing, Microelectron. Eng. 137 (2015) 124–129, https://doi.org/10.1016/j.mee.2015.02.003.
[54] F. Rigoni, S. Freddi, S. Pagliara, G. Drena, L. Suisse Sangaletti, J.-M. Bouvet, M. Malovichko, A.V. Bobrinetskiy Emelianov, Humidity enhanced sub-ppm sensitivity to ammonia of coalently functionalized single wall carbon nanotube bundle layers, Nanotechnology 28 (2017) 25552.
[55] L. Liu, X. Ye, K. Wu, R. Han, Z. Zhou, Humidity sensitivity of multi-walled carbon nanotube networks deposited by dielectrophoresis, Sensors 9 (2009) 1714–1721.